Galvanomagnetic Studies of Degenerate Gallium-Doped Germanium: Nonparabolic Energy Bands with Variable Warping

W. BERNARD, H. ROTH, AND W. D. STRAUB
Raytheon Research Division, Waltham, Massachusetts
(Received 23 May 1963)

Galvanomagnetic studies of degenerate p-type germanium are utilized to investigate the valence band structure at Fermi level penetrations up to 0.5 eV. Extensive resistivity and Hall measurements on a series of gallium-doped samples yield, for impurity concentrations $>5\times10^{19}$ cm^{-3}, apparent free-hole concentrations significantly in excess of the gallium concentrations as determined directly using several independent techniques. The experimentally observed disparity between the electrical and direct determinations of the gallium content can be accounted for by a detailed consideration of the valence band structure of germanium. Lax and Mavroides' treatment of the conductivity and Hall effect for parabolic, warped energy surfaces has been extended to include nonparabolic surfaces with variable warping. Application of this extended treatment to Kane's model of the multiple valence band structure of germanium satisfactorily predicts the observed departure of the Hall coefficient factor from unity over the impurity concentration range studied. The scattering relaxation time τ is deduced from a comparison of the measured and calculated values of the conductivity. An analysis of τ on the basis of screened impurity scattering in the Born approximation yields the observed energy dependence for $E<0.29$ eV. For $E>0.29$ eV a marked decrease in τ occurs, which is attributed to interband impurity scattering involving the split-off band. It is suggested that a pronounced temperature dependence observed in the resistivity for $T>80$°K arises from a corresponding temperature dependence of the electronic screening radius.

I. INTRODUCTION

IN recent years the energy band structures of various semiconducting materials have been studied extensively using galvanomagnetic effects, optical effects, and cyclotron resonance. As the experiments became more sophisticated it was found necessary in many cases to devise correspondingly more complex band structure models. Thus, for example, the multiple-ellipsoid conduction band and the warped two-valence band models of silicon and germanium were developed.[1,2] However, because the materials studied were relatively pure, the implications of the experimental results were limited primarily to the immediate vicinity of the band edges, where quadratic approximations to the energy spectra in k space are normally found to be adequate. In the meantime, considerable theoretical attention has been focused on the problem of extending the energy band description of semiconductors throughout larger regions of k space.[3] With the exception of optical studies,[4] however, which have yielded important information, predominantly at various symmetry points, little conclusive experimental evidence is available to test these theoretical extensions of the band theory.

Degenerate semiconductors furnish an ideal means for a more detailed, systematic investigation of the band structure at energies appreciably removed from the band edges. That the addition of degenerate concentrations of impurity atoms does not appear to introduce serious modifications in the shape of the energy surfaces is suggested by the theoretical treatments of Parmenter[5] and others,[6,7] according to which the principal effect is simply a uniform rigid energy displacement of the intrinsic band structure arising from the screened impurity ion potentials. A similar energy shift, arising from electron exchange, has recently been discussed by Wolff.[8] In addition, the random spatial distribution of impurities gives rise to tailing of the energy spectrum near the band edges. However, a relatively small fraction of the free carriers is contained in the band "tails" because of the low density-of-states in this region of the spectrum. The available experimental information with respect to degenerate semiconductors tends to support the above picture of the band structure. The optical work of Pankove[9] and of Fowler *et al.*[10] on bulk material indicates a slight shrinkage in the band gap, which may be attributed to band tailing. Recent infrared reflectivity studies[11,12] suggest that the effective masses are not appreciably modified in degenerate material. Extensive studies on tunnel diodes indicate that such diverse electrical properties as direct band-to-band

[1] C. Herring, Bell System Tech. J. **34**, 237 (1955).
[2] G. Dresselhaus, A. F. Kip, and C. Kittel, Phys. Rev. **98**, 368 (1955).
[3] See, for example, F. Herman, Rev. Mod. Phys. **30**, 102 (1958); also, J. Callaway, Solid State Phys. **7**, 99 (1958).
[4] For tabulations of some of the principal optical results, see J. C. Phillips, D. Brust, and F. Bassani, in *Proceedings of the International Conference on the Physics of Semiconductors, Exeter* (The Institute of Physics and the Physical Society, London, 1962), p. 564; and W. Paul and D. M. Warschauer, in *Solids Under Pressure* (McGraw-Hill Book Company, Inc., New York, 1963), Chap 8.
[5] R. H. Parmenter, Phys. Rev. **104**, 22 (1956).
[6] M. Lax and J. C. Phillips, Phys. Rev. **110**, 41 (1958).
[7] E. M. Conwell and D. W. Levinger, in *Proceedings of the International Conference on the Physics of Semiconductors, Exeter* (The Institute of Physics and the Physical Society, London, 1962), p. 227.
[8] P. A. Wolff, Phys. Rev. **126**, 405 (1962).
[9] J. I. Pankove and P. Aigrain, Phys. Rev. **126**, 956 (1962).
[10] A. B. Fowler, W. E. Howard, and C. E. Brock, Phys. Rev. **128**, 1664 (1962).
[11] W. G. Spitzer, F. A. Trumbore, and R. A. Logan, J. Appl. Phys. **32**, 1822 (1962).
[12] E. P. Rashevskaya and V. I. Fistul', Fiz. Tverd. Tela **4**, 2601 (1962) [translation: Soviet Phys.—Solid State **4**, 1907 (1963)].

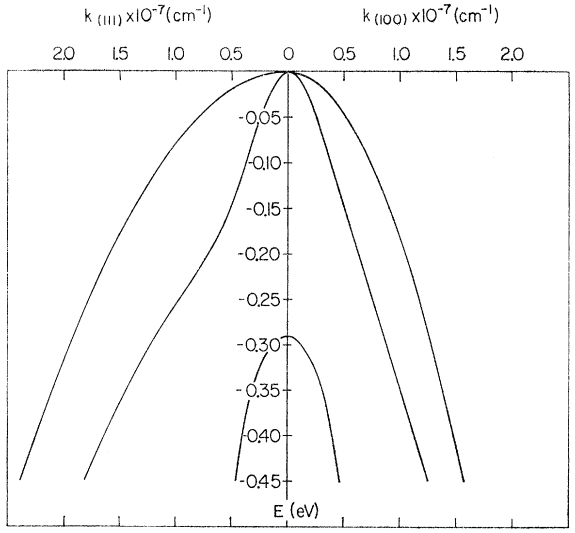

FIG. 1. E versus k curves based on Kane's three-valence band model of germanium, with $L=-30.7\hbar^2/2m_0$, $M=-5.8\hbar^2/2m_0$, $N=-33.0\hbar^2/2m_0$, and $\Delta=0.29$ eV. The heavy-hole band is parabolic and warped with respect to the [100] and [111] directions, while the light-hole band is nonparabolic with energy-dependent warping. The third band is that split off by the spin-orbit interaction Δ.

tunneling,[13,14] phonon-assisted tunneling,[15,16] pressure[17] and magnetic field[18] dependence of the tunneling current, and "excess current"[19–21] can be adequately accounted for on the basis of the intrinsic band structure.

While the experimental work performed to date on both bulk degenerate material and degenerate p-n junctions substantiates the close correspondence between the band structures of degenerate and intrinsic material, the results have not been sufficiently revealing to yield detailed information regarding the nature of the band structure away from the band edges. Cyclotron resonance, which has been of immense value in the clarification of intrinsic band properties, presents formidable problems in degenerate semiconductors arising from the extremely short relaxation times encountered. On the other hand, de Haas–Van Alphen effects, so useful in the study of metals, are not readily observable in most degenerate semiconductors. It would seem, therefore, that at present the most promising approach to the further study of the band structure of semiconductors at points appreciably removed from the band edges involves galvanomagnetic investigations of degenerate materials.

It is the purpose of the present paper to utilize galvanomagnetic studies of degenerate gallium-doped germanium to investigate the valence band structure at Fermi energy penetrations up to 0.5 eV, corresponding to impurity concentrations up to 5×10^{20} cm^{-3}. The basis for carrying out these studies is the existence of a striking experimental disparity between the electrical and direct determinations of the impurity content of the samples in the degenerate range.[22] Trumbore and Tartaglia[23] first pointed out that at the higher doping levels, Hall concentrations, assuming the degenerate formula $p=1/Re$, appeared to be larger than the corresponding chemical concentrations, but doubted that the effect was real, owing to large experimental errors. Similar observations and conclusions were noted by McCaldin and Wittry.[24] In order to examine this question more carefully we have performed extensive resistivity and Hall measurements on a series of degenerate p-type germanium samples and have found that, for impurity concentrations $>5\times10^{19}$ cm^{-3}, the apparent free-hole concentrations are significantly in excess of the gallium concentrations as determined directly using several independent techniques.[25] That is, the Hall coefficient factor $r=N_aRe$ is substantially less than unity, where N_a is the *true* impurity concentration.

It is well known that in nondegenerate material deviations of the Hall coefficient factor from unity can be related to the detailed form of the energy surfaces, as well as to the scattering mechanism. In particular, departures from spherical energy surfaces tend to decrease r, as in the case of the many-valley ellipsoid model of the germanium conduction band.[1] Similarly, Lax and Mavroides[26] have examined the parabolic, warped two-valence band model of Dresselhaus, Kip, and Kittel[27] and have shown that the effect of warping of the energy surfaces is a reduction in the Hall coefficient factor for Boltzmann statistics. In germanium, for example, ignoring the scattering contribution, the Hall coefficient factor of the heavy-hole band alone is predicted to be 0.77. On the other hand, the effect of combining the two warped bands is to yield a net r substantially >1, a result which has been observed experimentally by Morin[28] and studied extensively by Beer and Willardson[29] in nondegenerate material. Since experimentally

[13] L. Esaki, Phys. Rev. **109**, 603 (1959).
[14] E. O. Kane, J. Appl. Phys. **32**, 83 (1961).
[15] L. V. Keldysh, Zh. Eksperim. i Teor. Fiz. **34**, 962 (1958) [translation: Soviet Phys.—JETP **7**, 665 (1958)].
[16] N. Holanyak, I. A. Lesk, R. N. Hall, J. J. Tiemann, and H. Ehrenreich, Phys. Rev. Letters **3**, 167 (1959).
[17] S. L. Miller, M. I. Nathan, and A. C. Smith, Phys. Rev. Letters **4**, 60 (1960).
[18] A. R. Calawa, R. H. Rediker, B. Lax, and A. L. McWhorter, Phys. Rev. Letters **5**, 55 (1960).
[19] C. T. Sah, Phys. Rev. **123**, 1594 (1961).
[20] A. G. Chynoweth, W. L. Feldman, and R. A. Logan, Phys. Rev. **121**, 684 (1961).
[21] R. S. Claassen, J. Appl. Phys. **32**, 2372 (1961).
[22] H. Roth, W. D. Straub, and R. Tramposch, Bull. Am. Phys. Soc. **7**, 174 (1962).
[23] F. A. Trumbore and A. A. Tartaglia, J. Appl. Phys. **29**, 1511 (1958).
[24] J. O. McCaldin and D. B. Wittry, J. Appl. Phys. **32**, 65 (1961).
[25] W. Bernard, H. Roth, and W. D. Straub, Bull. Am. Phys. Soc. **8**, 224 (1963).
[26] B. Lax and J. G. Mavroides, Phys. Rev. **100**, 1650 (1955), henceforth referred to as LM.
[27] G. Dresselhaus, A. F. Kip, and C. Kittel, Phys. Rev. **98**, 368 (1955); henceforth referred to as DKK.
[28] F. J. Morin, Phys. Rev. **93**, 62 (1954).
[29] A. C. Beer and R. K. Willardson, Phys. Rev. **110**, 1286 (1958).

we observe a substantial decrease in r as the Fermi level penetrates the valence band, the energy surfaces must exhibit a more complex form away from the band edges. We assume, of course, that the LM results are valid in the case of degenerate statistics, and that the effect can be accounted for on the basis of band structure considerations alone.

The calculation of Kane[30] for the valence band structure of germanium is of particular interest in that portion of k space with which we are concerned. In Fig. 1 we have used the results of Kane's calculation to plot E versus k curves for the germanium valence bands. We note that as the bands are penetrated, the light hole band becomes nonparabolic and its warping energy dependent. In order to incorporate a complex band structure of this type in the analysis of our experimental results, it is necessary to extend the LM treatment of galvanomagnetic effects in warped, parabolic energy bands to the case of nonparabolic bands with variable warping. That the Hall coefficient anomaly can be satisfactorily accounted for in this way is strong confirmation of the validity of the Kane model. This result, in turn, enables us to examine in some detail various aspects of the scattering processes in degenerate p-type germanium.

We first present in Sec. II a comprehensive discussion of our experimental results. Section III is devoted to the extension of the LM calculation of galvanomagnetic effects to include nonparabolic bands with variable warping. In Sec. IV we incorporate Kane's valence band model into the formalism, and a theoretical prediction of the Hall coefficient factor as a function of impurity concentration is obtained. Finally, in Sec. V, the concentration and temperature dependence of the relaxation time is examined, and the relevant scattering mechanisms are discussed.

II. EXPERIMENTAL

A series of gallium-doped germanium single crystals was grown in our laboratory with concentrations ranging up to the solid solubility limit[31] of approximately 5×10^{20} cm^{-3}. Although the crystals were grown by both the horizontal zone and Czochralski techniques from seeds oriented in the [111], [110], and [100] crystallographic directions, no correlation between these parameters and the experimental results was observed.

Each sample was cut ultrasonically into a standard six-arm bridge configuration with approximate dimensions 10 mm$\times$2 mm$\times$1 mm, sandblasted, and subsequently etched in CP-4. Five electrical contacts were attached to each sample by bonding 3-mil gallium (1%) gold wires, providing current, resistivity, and Hall probes.

Hall effect and resistivity measurements were carried out in a stainless steel liquid helium research Dewar suspended in a 12-in. electromagnet having tapered pole pieces with a 1.4-in. air gap. A careful magnetic field calibration was made from 100 G to 20 kG with a Rawson-Lush rotating coil gaussmeter, type 820, accurate to 0.1%. Current through the sample was supplied by a Princeton Applied Research Model TC-602R constant-voltage source modified to provide an adjustable current stable to one part in 10^5. Potential measurements were made with a Type 150R Keithley voltmeter and monitored with a Leeds and Northrup continuous single point recorder. A multiple potential divider permitted the ultimate calibration of the recorder-voltmeter system on all ranges to better than $\pm0.2\%$ of full scale. Measurements of temperature dependence were performed in a Dewar of large thermal mass, which incorporated means for sensitive temperature control. The temperature was monitored with a calibrated[32] platinum resistance thermometer.

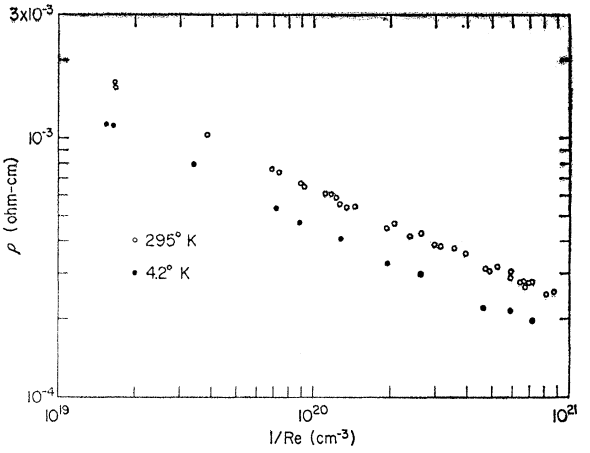

FIG. 2. Resistivity versus $1/Re$ for degenerate gallium-doped germanium samples studied. Results are shown for the two temperatures 4.2 and 295°K.

During the course of the measurements, we observed the standard precautions associated with galvanomagnetic studies such as magnetic field and current reversal, sample orientation with respect to magnetic field, and current-voltage linearity. These precautions eliminate all extraneous thermogalvanomagnetic effects with the exception of the Ettingshausen effect. However, calculations based on standard formulas for metals,[33] suitably corrected for the modification of the Wiedemann-Franz ratio in degenerate semiconductors,[34] indicate that the Ettingshausen contribution to the Hall signal should be completely negligible at helium temperature and $<1\%$ at room temperature, except possibly for the lowest impurity concentrations considered.

A summary of all resistivity and Hall investigations performed at 295 and 4.2°K is presented in Fig. 2. The

[30] E. O. Kane, J. Phys. Chem. Solids **1**, 82 (1956).
[31] F. A. Trumbore, Bell System Tech. J. **39**, 205 (1960).
[32] M. G. Holland, L. G. Rubin and J. Welts, *Temperature—Its Measurement and Control in Science and Industry* (Reinhold Publishing Corporation, New York, 1962), Vol. 3, Part 2, p. 795.
[33] A. H. Wilson, *Theory of Metals* (Cambridge University Press, Cambridge, England, 1954), 2nd ed., Chap. 8.
[34] E. H. Putley, Proc. Phys. Soc. (London) **B65**, 991 (1952).

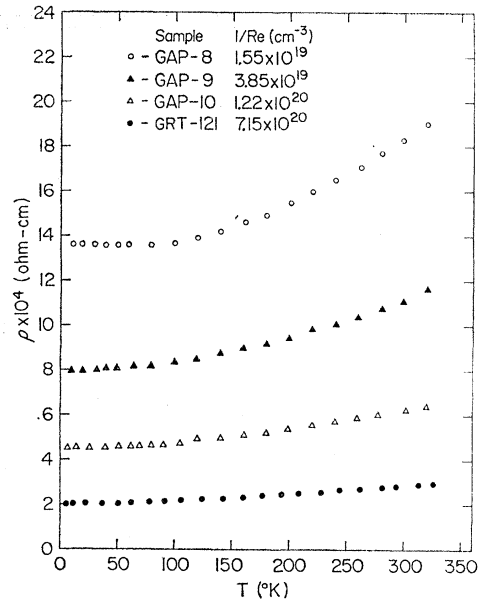

FIG. 3. Temperature dependence of the resistivity for several representative samples of gallium-doped germanium.

experimental scatter is of the order of $\pm 3\%$, which is that expected from the total estimated possible errors arising from both instrumentation and measurements of sample dimensions. The possibility that sample inhomogeneities contribute significant errors to these measurements is thus essentially eliminated by the lack of excessive experimental scatter. The fact that the samples were prepared from numerous crystals grown in different orientations and by two different techniques is further evidence in support of this conclusion. The possibility that the presence of dislocations affects the electrical transport properties was also investigated. Hall and resistivity measurements performed prior and subsequent to the addition of dislocations by bending a sample near its melting point resulted in no observable change.

The temperature dependence of the resistivity for several representative samples is shown in Fig. 3. The experimental results presented in Figs. 2 and 3 will form the basis for an analysis of the scattering processes appropriate to these materials, and will be discussed in detail in Sec. V.

It is clear that an essential element in the present study is the accurate determination of the Hall coefficient. Consequently, both magnetic field and temperature dependences were carefully investigated to ensure that each sample could be characterized by a unique Hall coefficient. Typical results of the magnetic field dependence of the reciprocal Hall coefficient are exhibited in Fig. 4. With the possible exception of the low-field values, where the signals in the most highly doped samples are fractions of microvolts, the experimental scatter is of the order of $\pm 0.5\%$. We note that the measurements of all samples were performed in the low magnetic field limit $\mu H \ll 1$, and, hence, no variation with field is to be expected.

Figure 5 shows the temperature dependence of the reciprocal Hall coefficient for typical samples in the range from liquid helium to room temperature. Except for the sample with the smallest concentration, which appears to exhibit an 8% rise at higher temperatures, the Hall concentration is temperature-independent to within $\pm 3\%$. Because the Hall coefficient is largely insensitive to temperature, we shall use room-temperature values throughout the following discussion.

In order to provide a direct determination of the Hall coefficient factor of our samples, it was necessary to obtain the actual gallium concentrations. Three independent methods were utilized to achieve this objective, viz., spectrographic, neutron activation, and complexometric titration analyses. These procedures are described in brief below.

Spectrographic analysis was carried out by the Jarrell Ash Company of Newton, Massachusetts. The procedure involved the dissolution of the sample and an equal weight of indium in nitric and hydrofluoric acids and the subsequent dilution with water. An emission spectrum was obtained with a plane grating spectrograph (3.4-m focal length) using the solution spark technique incorporating a rotating disk electrode. Sensitive spectral lines of gallium and indium were selected for several concentration ranges and analyzed with the aid of a densitometer. The relative line intensities were compared to carefully prepared standards and each gallium concentration deduced from a set of three determinations.

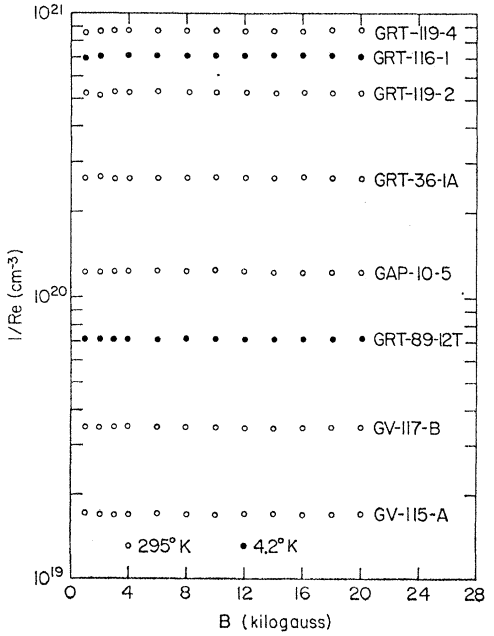

FIG. 4. Magnetic field dependence of the Hall concentration $1/Re$ for representative samples of gallium-doped germanium.

Neutron activation analysis was performed by the General Atomic Division of General Dynamics Corporation. The analytical procedure involved irradiation of the sample and a gallium standard in a thermal neutron flux. After decay of short-lived interfering activities, the gamma-ray spectra of sample and standard were taken. The gallium concentration was determined by comparing the relative intensities of a suitably selected gamma ray.

Complexometric determination of gallium in germanium was carried out in our laboratory using EDTA titration. The samples were dissolved in aqua regia, the excess nitric acid destroyed with urea, and the gallium extracted with ether using standard procedures. Excess zinc-EDTA complex was added under controlled conditions of pH and temperature. Using Zincon as indicator, the solution was titrated with EDTA to a sharp yellow end point and the gallium concentration thus obtained. All solutions were standardized against a primary gallium and a secondary zinc standard.

The gallium concentration determinations N_a provided by the various methods, in conjunction with the electrically determined Hall concentrations $1/Re$, lead directly to the evaluation of the Hall coefficient factor $r=N_aRe$ as a function of doping level. The results in Fig. 6 display the relationship between the Hall coefficient factor and $1/Re$. In comparison to the previously discussed case of the Hall concentrations, the experimental uncertainties of the direct gallium determinations are rather difficult to assess. Although individual internal consistencies are better than $\pm 5\%$, it is seen that the absolute errors inherent in a given technique can be somewhat larger. Because the three independent methods yield results which are in substantial agreement, however, it is clear that we have obtained a reliable quantitative statement of the Hall coefficient anomaly.

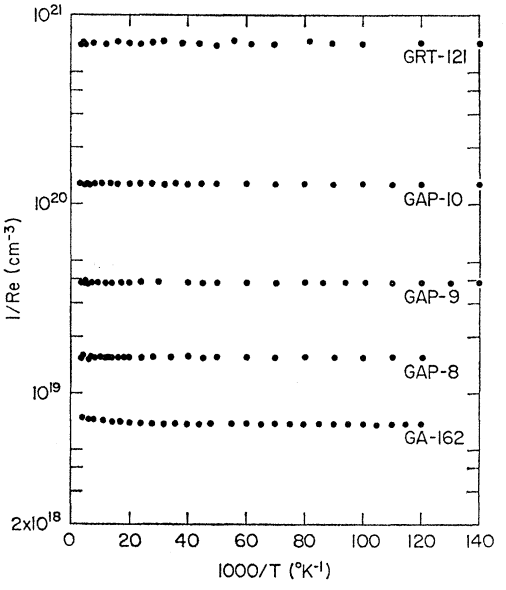

FIG. 5. Temperature dependence of the Hall concentration $1/Re$ for representative samples of gallium-doped germanium.

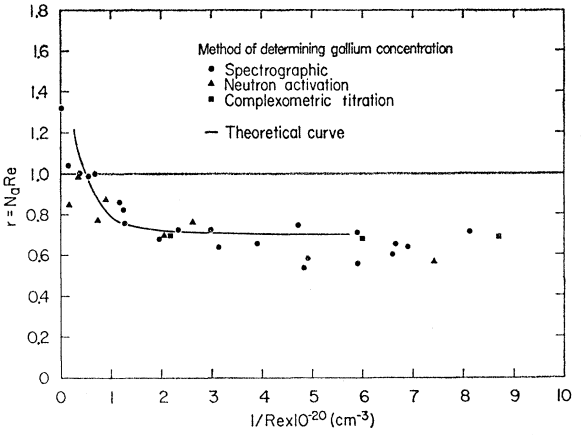

FIG. 6. Hall coefficient factor of degenerate, gallium-doped germanium as a function of Hall concentration $1/Re$. The various techniques used for the direct determination of the gallium concentration are indicated. The theoretical prediction is the result of an analysis based on the actual valence band structure of germanium taking into account nonparabolicity and energy-dependent warping.

It is seen from Fig. 6 that, at low concentrations, the Hall coefficient factor $r>1$ and is approaching its nondegenerate value. As $1/Re$ increases, r monotonically decreases, becoming significantly <1 for $1/Re>5\times10^{19}$ cm^{-3}. These results form the basis for our investigation of the valence band structure of degenerate p-type germanium.

III. GALVANOMAGNETIC COEFFICIENTS IN NONPARABOLIC BANDS WITH VARIABLE WARPING

In this section we derive general formulas from which the free carrier concentration p, the conductivity σ, and the Hall conductivity $\sigma^{(H)}$ can be calculated for nonparabolic energy bands with variable warping. In terms of these quantities, the Hall coefficient for a single band is

$$R=-\sigma^{(H)}/\sigma^2, \tag{1}$$

and the Hall coefficient factor r, which expresses the ratio of the *true* concentration of free carriers to $1/Re$ is

$$r=peR=-ep\sigma^{(H)}/\sigma^2. \tag{2}$$

In the case of a two-band model

$$r=-e(p_h+p_l)(\sigma_h^{(H)}+\sigma_l^{(H)})/(\sigma_h+\sigma_l)^2. \tag{3}$$

Because the transport integrals appropriate to the bands considered here cannot be evaluated in closed form, we extend the series expansion technique developed for the case of parabolic bands with constant warping by LM.[26] The $T\rightarrow 0$ approximation, appropriate to degenerately doped semiconductors, will be adopted throughout.

We assume an energy spectrum for holes of the form

$$E(\mathbf{k})=G(K^2), \tag{4}$$

where $G(K^2)$ is a general monotonically increasing function of

$$K^2=k^2\{1+b(E)\times[1+c^2(k_x^2k_y^2+k_y^2k_z^2+k_z^2k_x^2)/k^4]^{1/2}\}. \tag{5}$$

The nonparabolicity of the band is implicit in the functional dependence of G on K^2, while the functional dependence of b on E implies a variation of the warping with energy. For $G(K^2)\rightarrow AK^2$ and $b\rightarrow\pm B/A$, Eqs. (4) and (5) reduce to the parabolic, warped valence bands of DKK.[27] We will also make use of the LM approximation to K^2,

$$K^2\simeq a(E)k^2[1+\gamma(E)q], \tag{6}$$

in which only the first two terms of the expansion in powers of

$$q=\tfrac{1}{6}-(k_x^2k_y^2+k_y^2k_z^2+k_z^2k_x^2)/k^4 \tag{7}$$

are retained. In Eq. (6)

$$a(E)=[1+b(E)(1+\tfrac{1}{6}c^2)^{1/2}], \tag{8}$$

and

$$\gamma(E)=-\frac{b(E)c^2}{2a(E)(1+\frac{1}{6}c^2)^{1/2}}. \tag{9}$$

We next consider the general expressions for the free hole concentration p, the conductivity σ, and the Hall conductivity $\sigma^{(H)}$ in crystals exhibiting cubic symmetry. With the assumption of degenerate statistics, these can be written in spherical coordinates as

$$p=\frac{1}{12\pi^3}\int_0^{2\pi}d\varphi\int_0^{\pi}d\theta k^3\sin\theta, \tag{10}$$

$$\sigma=\frac{e^2\tau}{4\pi^3\hbar^2}\int_0^{2\pi}d\varphi\int_0^{\pi}d\theta\sin\theta\frac{k^3(\partial E/\partial k_x)^2}{\mathbf{k}\cdot\nabla_k E(\mathbf{k})}, \tag{11}$$

and

$$\sigma^{(H)}=-\frac{e^3\tau^2}{4\pi^3\hbar^4}\int_0^{2\pi}d\varphi\int_0^{\pi}d\theta\sin\theta\frac{k^3}{\mathbf{k}\cdot\nabla_k E(\mathbf{k})}\times\left[\left(\frac{\partial E}{\partial k_y}\right)^2\frac{\partial^2E}{\partial k_x^2}-\frac{\partial E}{\partial k_y}\frac{\partial E}{\partial k_x}\frac{\partial^2E}{\partial k_y\partial k_x}\right]. \tag{12}$$

The angular integrations are to be performed over the Fermi surface as determined by Eqs. (4) and (5). Since we wish to focus our attention on the implications of band structure with respect to the galvanomagnetic effects, we have assumed the scattering relaxation time τ to be a function of the energy alone.

We recall the LM technique for evaluating the transport integrals by considering the free hole concentration p, which is formally unaffected by either the lack of parabolicity or the energy dependence of the warping, since it is determined simply by the volume in k space enclosed by the Fermi surface. Substituting for k^3 from Eq. (6), Eq. (10) becomes

$$\begin{aligned}p&=\frac{K^3}{12\pi^3a^{3/2}}\int_0^{2\pi}d\varphi\int_0^{\pi}d\theta\sin\theta(1+\gamma q)^{-3/2}\\&=\frac{K^3}{12\pi^3a^{3/2}}\int_0^{2\pi}d\varphi\int_0^{\pi}d\theta\\&\quad\times\sin\theta\left(1-\frac{3}{2}\gamma q+\frac{15}{8}\gamma^2q^2-\frac{35}{16}\gamma^3q^3+\cdots\right),\end{aligned} \tag{13}$$

where we note that K^3 is a constant over the Fermi surface. Expressing q, Eq. (7) ,in spherical coordinates and carrying out the indicated angular integrations, we obtain

$$p=(K^3/3\pi^2a^{3/2})\times(1+0.05\gamma+0.01635\gamma^2+0.000908\gamma^3+\cdots). \tag{14}$$

In order to include the nonparabolicity and the energy dependence of the warping in a tractable way, we wish to separate these effects from that of the warping alone in the differential operations on $E(\mathbf{k})$ appearing in Eqs. (11) and (12). Differentiation of Eqs. (4) and (5) with respect to k_x yields

$$\frac{\partial E}{\partial k_x}=\frac{dG}{d(K^2)}\left[\frac{D(K^2)}{Dk_x}+\frac{db}{dE}\frac{\partial E}{\partial k_x}\Lambda^2\right], \tag{15}$$

where D/Dk_x denotes an explicit partial derivative with respect to k_x, and

$$\Lambda^2=k^2[1+c^2(k_x^2k_y^2+k_y^2k_z^2+k_z^2k_x^2)/k^4]^{1/2}. \tag{16}$$

Solving for $\partial E/\partial k_x$, we obtain

$$\frac{\partial E}{\partial k_x}=\frac{dG}{d(K^2)}\frac{D(K^2)}{Dk_x}\Big/\left(1-\frac{db}{dE}\frac{dG}{d(K^2)}\Lambda^2\right). \tag{17}$$

By performing second differentiations of Eqs. (4) and (5) for E and invoking Eq. (17), it is possible to obtain analogous expressions for $\partial^2E/\partial k_x^2$ and $\partial^2E/\partial k_x\partial k_y$. It is shown in Appendix A that this procedure leads for cubic symmetry to the relatively simple result

$$\left(\frac{\partial E}{\partial k_y}\right)^2\frac{\partial^2E}{\partial k_x^2}-\frac{\partial E}{\partial k_x}\frac{\partial E}{\partial k_y}\frac{\partial^2E}{\partial k_x\partial k_y}=\left\{\frac{dG}{d(K^2)}\Big/\left(1-\frac{db}{dE}\frac{dG}{d(K^2)}\Lambda^2\right)\right\}^3\times\left\{\left[\frac{D(K^2)}{Dk_y}\right]^2\frac{D^2(K^2)}{Dk_x^2}-\frac{D(K^2)}{Dk_x}\frac{D(K^2)}{Dk_y}\frac{D^2(K^2)}{Dk_xDk_y}\right\}. \tag{18}$$

Substitution of Eqs. (17) and (18) into Eqs. (11) and (12) yields σ and $\sigma^{(H)}$ in the form

$$\sigma=\frac{e^2\tau}{4\pi^3\hbar^2}\frac{dG}{d(K^2)}\int_0^{2\pi}d\varphi\int_0^{\pi}d\theta k^3\sin\theta\left[\frac{D(K^2)}{Dk_x}\right]^2\Big/\left\{\left[k_x\frac{D(K^2)}{Dk_x}+k_y\frac{D(K^2)}{Dk_y}+k_z\frac{D(K^2)}{Dk_z}\right]\left[1-\frac{db}{dE}\frac{dG}{d(K^2)}\Lambda^2\right]\right\} \tag{19}$$

and

$$\sigma^{(H)}=-\frac{e^3\tau^2}{4\pi^3\hbar^4}\left[\frac{dG}{d(K^2)}\right]^2\int_0^{2\pi}d\varphi\int_0^{\pi}d\theta\frac{k^3\sin\theta\left\{\left[\frac{D(K^2)}{Dk_y}\right]^2\frac{D^2(K^2)}{Dk_x^2}-\frac{D(K^2)}{Dk_x}\frac{D(K^2)}{Dk_y}\frac{D^2(K^2)}{Dk_xDk_y}\right\}}{\left[k_x\frac{D(K^2)}{Dk_y}+k_y\frac{D(K^2)}{Dk_y}+k_z\frac{D(K^2)}{Dk_z}\right]\left[1-\frac{db}{dE}\frac{dG}{d(K^2)}\Lambda^2\right]^2}. \tag{20}$$

Noting, since K^2 is explicitly a homogeneous second-order function of k_x, k_y, k_z, that

$$\left[k_x\frac{D(K^2)}{Dk_x}+k_y\frac{D(K^2)}{Dk_y}+k_z\frac{D(K^2)}{Dk_z}\right]=2K^2,$$

and substituting for k^3 from Eq. (6), Eqs. (19) and (20) become

$$\sigma=\frac{e^2\tau K^3}{8\pi^3\hbar^2a^{3/2}}\frac{dG}{d(K^2)}\int_0^{2\pi}d\varphi\int_0^{\pi}d\theta\sin\theta\left(\frac{1}{K^2}\left[\frac{D(K^2)}{Dk_x}\right]^2\Big/\left\{[1+\gamma q]^{3/2}\left[1-\frac{db}{dE}\frac{dG}{d(K^2)}\Lambda^2\right]\right\}\right) \tag{21}$$

and

$$\sigma^{(H)}=-\frac{e^3\tau^2K^3}{8\pi^3\hbar^4a^{3/2}}\left[\frac{dG}{d(K^2)}\right]^2\int_0^{2\pi}d\varphi\int_0^{\pi}d\theta$$
$$\times\sin\theta\left(\frac{1}{K^2}\left\{\left[\frac{D(K^2)}{Dk_y}\right]^2\frac{D^2(K^2)}{Dk_x^2}-\frac{D(K^2)}{Dk_x}\frac{D(K^2)}{Dk_y}\frac{D^2(K^2)}{Dk_xDk_y}\right\}\Big/\left\{[1+\gamma q]^{3/2}\left[1-\frac{db}{dE}\frac{dG}{d(K^2)}\Lambda^2\right]^2\right\}\right). \tag{22}$$

Using Eq. (6) for K^2, the quantities $(1/K^2)[D(K^2)/Dk_x]^2$ and

$$(1/K^2)\{[D(K^2)/Dk_y]^2[D^2(K^2)/Dk_x^2]-[D(K^2)/Dk_x][D(K^2)/Dk_y][D^2(K^2)/Dk_xDk_y]\}$$

are found to be polynomials in γ, the coefficients of which are functions of the angular coordinates only. We point out that Eqs. (21) and (22) differ from the LM result in two important and straightforward respects. The effect of the nonparabolicity enters simply through the quantity $dG/d(K^2)$, which replaces A outside the integrals, while the energy dependence of the warping gives rise to the correction factors $\{1-(db/dE)[dG/d(K^2)]\Lambda^2\}^{-1}$ in the integrands.

The quantity Λ^2 appearing in Eqs. (21) and (22), like K^2 in Eq. (5), can be approximated by the first two terms of an expansion in powers of q:

$$\Lambda^2\simeq a'k^2(1-\gamma'q), \tag{23}$$

where

$$a'=(1+\tfrac{1}{6}c^2)^{1/2},\quad \gamma'=c^2/2(1+\tfrac{1}{6}c^2). \tag{24}$$

Using Eq. (23), together with Eq. (6) for k^2, we obtain

$$\left[1-\frac{db}{dE}\frac{dG}{d(K^2)}\Lambda^2\right]=\frac{a''(1+\Gamma q)}{(1+\gamma q)}, \tag{25}$$

where

$$a''=1-\frac{db}{dE}\frac{dG}{d(K^2)}\frac{a'}{a}K^2, \tag{26}$$

and

$$\Gamma=\frac{\gamma}{a''}\left[1+\frac{db}{dE}\frac{dG}{d(K^2)}\frac{a'\gamma'}{a\gamma}K^2\right]. \tag{27}$$

For $db/dE<0$, which as will be seen in Sec. IV, is satisfied by Kane's valence band model of germanium, Γ is typically of the same order of magnitude as γ. In fact, as the warping becomes energy-independent, $db/dE\to 0$, $a''\to 1$, and $\Gamma\to\gamma$. We also note in this connection that the requirement $\partial E/\partial k>0$ in every direction in k space

is approximated by the condition $a''>0$. Substituting Eq. (25) into Eqs. (21) and (22), we have the results

$$\sigma=\frac{e^2\tau K^3}{8\pi^3\hbar^2a^{3/2}a''}\frac{dG}{d(K^2)}\int_0^{2\pi}d\varphi\int_0^{\pi}d\theta\sin\theta\left\{\frac{1}{K^2}\left[\frac{D(K^2)}{Dk_x}\right]^2\Big/(1+\gamma q)^{1/2}(1+\Gamma q)\right\} \tag{28}$$

and

$$\sigma^{(H)}=-\frac{e^3\tau^2K^3}{8\pi^3\hbar^4a^{3/2}a''^2}\left[\frac{dG}{d(K^2)}\right]^2\int_0^{2\pi}d\varphi\int_0^{\pi}d\theta \times\sin\theta\left(\frac{1}{K^2}\left\{\left[\frac{D(K^2)}{Dk_y}\right]^2\frac{D^2(K^2)}{Dk_x^2}-\frac{D(K^2)}{Dk_x}\frac{D(K^2)}{Dk_y}\frac{D^2(K^2)}{Dk_xDk_y}\right\}\Big/[(1+\gamma q)^{-1/2}(1+\Gamma q)^2]\right). \tag{29}$$

We now obtain approximate evaluations of the transport integrals in Eqs. (28) and (29) by expanding the quantities

$$[(1+\gamma q)^{-1/2}(1+\Gamma q)^{-1}] \quad\text{and}\quad [(1+\gamma q)^{1/2}(1+\Gamma q)^{-2}],$$

respectively, in powers of q and performing the indicated angular integrations. The resulting series for σ and $\sigma^{(H)}$ can be written in the form

$$\sigma=\frac{2e^2\tau K^3}{3\pi^2\hbar^2a^{1/2}a''}\frac{dG}{d(K^2)}(1+x_1+x_2+x_3+x_4+x_5+\cdots) \tag{30}$$

and

$$\sigma^{(H)}=-\frac{4e^3\tau^2K^3a^{1/2}}{3\pi^2\hbar^4a''^2}\left[\frac{dG}{d(K^2)}\right]^2 \times(1+y_1+y_2+y_3+y_4+\cdots), \tag{31}$$

where the detailed expressions for the indicated terms of the series are given below in Table I. It is seen that the terms have been grouped such that each nth-order term is of the form

$$\sum_{m=0}^{n}\nu_{nm}\gamma^m\Gamma^{n-m}.$$

In the limit of constant warping $\Gamma\to\gamma$, and the series reduce to those obtained by LM. We have explicitly evaluated the series for each transport integral to the order indicated by LM.

TABLE I. Series expansion terms for the quantities σ and $\sigma^{(H)}$

Term in series	Explicit evaluation in terms of γ and Γ
x_1	$-0.01667\gamma+0.03333\Gamma$
x_2	$0.03701\gamma^2-0.00437\gamma\Gamma+0.00873\Gamma^2$
x_3	$0.000440\gamma^3+0.000259\gamma^2\Gamma-0.000208\gamma\Gamma^2+0.000415\Gamma^3$
x_4	$0.000373\gamma^4+0.000294\gamma^3\Gamma+0.000185\gamma^2\Gamma^2$ $-0.000067\gamma\Gamma^3+0.000135\Gamma^4$
x_5	$0.0000063\gamma^5+0.0000053\gamma^4\Gamma+0.0000040\gamma^3\Gamma^2$ $+0.0000021\gamma^2\Gamma^3-0.0000034\gamma\Gamma^4+0.0000069\Gamma^5$
y_1	$-0.08333\gamma+0.06667\Gamma$
y_2	$-0.04078\gamma^2+0.03255\gamma\Gamma+0.02619\Gamma^2$
y_3	$-0.007090\gamma^3-0.000308\gamma^2\Gamma-0.001250\gamma\Gamma^2$ $+0.001662\Gamma^3$
y_4	$0.0002480\gamma^4+0.0012310\gamma^3\Gamma-0.001962\gamma^2\Gamma^2$ $+0.001070\gamma\Gamma^3+0.0006739\Gamma^4$

Before proceeding to apply the above results to the valence bands of germanium, it is of interest to comment briefly on their implications with respect to nonparabolic, spherically symmetric bands. Suppose, for example, we attempt to approximate the germanium valence bands by neglecting the warping, but allowing the bands to deviate from parabolicity as the energy penetration is increased. The results can be most directly obtained by considering Eqs. (14), (30), and (31). Since $b=0$, then $a=a''=1$, $\gamma=\Gamma=0$, and all series expansions reduce to unity. Using Eq. (2) for the Hall coefficient factor r, it is apparent that for a single, nonparabolic band $r\equiv1$, so that $p\equiv1/Re$.[35] For a spherically symmetric two-band model, we find, using Eq. (3) for r, that

$$r=\frac{\{p_h+p_l\}\left\{p_h\left[\frac{dG_h}{d(K^2)}\right]^2+p_l\left[\frac{dG_l}{d(K^2)}\right]^2\right\}}{\left\{p_h\frac{dG_h}{d(K^2)}+p_l\frac{dG_l}{d(K^2)}\right\}^2}. \tag{32}$$

It can be seen that $r\geq1$ for such a model by rewriting Eq. (32) in the form

$$r=1+p_hp_l\frac{\left[\frac{dG_h}{d(K^2)}-\frac{dG_l}{d(K^2)}\right]^2}{\left[p_h\frac{dG_h}{d(K^2)}+p_l\frac{dG_l}{d(K^2)}\right]^2}\geq1. \tag{33}$$

[35] The result $p\equiv1/Re$ for a single, spherically symmetric, degenerate band is also of interest in connection with the theory of metals. In a number of texts on the band structure and transport properties of solids, a commonly advanced simple explanation for the anomalous positive Hall effect exhibited by certain metals assumes a reversal of the Hall voltage at inflection points of the energy bands in k space. That is, it is assumed that when a (spherically symmetric) conduction band is filled with electrons beyond an inflection point, one is concerned with holes, and thus, the Hall effect becomes positive. It is evident from Eq. (31) that the Hall effect for a nonparabolic spherical band does not in fact change sign at an inflection point. The reader can quickly convince himself on this question by applying Eq. (12) to a simple energy band, for example, of the form $E(k)=Ak^2-Bk^4$. Thus, the above simple criterion cannot be applied to the choice between electronic and hole conduction, and the explanation for the anomalous Hall effect in metals must rest on more subtle band structure considerations.

IV. THE VALENCE BAND STRUCTURE OF GERMANIUM AND THE HALL COEFFICIENT FACTOR ANOMALY

Having derived an approximate formalism for the calculation of p, σ, and $\sigma^{(H)}$ in nonparabolic energy bands with variable warping, we now consider explicitly the valence band structure of germanium. The most detailed calculation available over the region of k space with which we are concerned appears to be that due to Kane,[30] who extended the parabolic, warped, two-band model of DKK[27] by assuming that the energy measured from $k=0$ is not necessarily small compared to the spin-orbit splitting.

Since the split-off band, as well as the familiar light- and heavy-hole bands, is involved, Kane obtains a third-order secular equation for the energy. Although it is necessary to solve the secular equation numerically for an arbitrary direction in k space, it is possible to obtain explicit solutions for the three energy bands in the [100] and [111] directions. In the [100] direction the heavy-hole band has the form

$$E_h^{[100]}=(A-B)k^2, \tag{34}$$

while the light-hole band E_l and the split-off band E_Δ have the form

$$E_{l,\Delta}^{[100]}=\tfrac{1}{2}\{(2A+B)k^2+\Delta\}\mp\tfrac{1}{2}\{[(2A+B)k^2+\Delta]^2 -4\Delta(A+B)k^2-4(A+2B)(A-B)k^4\}^{1/2}. \tag{35}$$

The $-$ and $+$ signs correspond to the light-hole band and the split-off band, respectively. In the [111] direction we have

$$E_h^{[111]}=[A-(B^2+\tfrac{1}{3}C^2)^{1/2}]k^2 \tag{36}$$

and

$$E_{l,\Delta}^{[111]}=\tfrac{1}{2}\{[2A+(B^2+\tfrac{1}{3}C^2)^{1/2}]k^2+\Delta\} \mp\tfrac{1}{2}\{([2A+(B^2+\tfrac{1}{3}C^2)^{1/2}]k^2+\Delta)^2 -4\Delta[A+(B^2+\tfrac{1}{3}C^2)^{1/2}]k^2 -4[A+2(B^2+\tfrac{1}{3}C^2)^{1/2}] \times[A-(B^2+\tfrac{1}{3}C^2)^{1/2}]k^4\}^{1/2}. \tag{37}$$

The E versus k curves obtained from Eqs. (34) through (37) have previously been introduced in Fig. 1. The value assumed for the spin-orbit splitting, as found by Kane to yield the best agreement with optical data, was $\Delta=0.29$ eV. The values selected for the other valence band parameters were $A=13.1\hbar^2/2m_0$, $B=8.3\hbar^2/2m_0$, and $C=12.5\hbar^2/2m_0$, as obtained by Dexter, Zeiger, and Lax from cyclotron resonance experiments.[36] According to Eqs. (34) and (36) the heavy-hole band is parabolic with constant warping in the [100] and [111] directions. On the other hand, it is seen from Eqs. (35) and (37) that the light-hole band exhibits a departure from parabolicity and a change in warping as the band is penetrated, such that at large energies it becomes identical with the heavy-hole band except for a constant energy displacement. In the [110] direction, which is not shown in Fig. 1, the heavy-hole band, as well as the light-hole band, deviates from parabolicity. The E versus k curves for the two bands in the [110] direction lie between their respective E versus k curves in the [100] and [111] directions.

We note that the Fermi surface intersects the split-off band, which is also shown in Fig. 1, for hole concentrations $\gtrsim 1.8\times10^{20}$ cm^{-3}. Because this band contains $<1\%$ of the total carriers for the highest impurity concentrations considered, however, it will not be explicitly included in our calculation of the galvanomagnetic effects. This approximation appears to be a valid one, since the experimental results can be satisfactorily accounted for using the two-band model. Although the direct contribution of the split-off band to the conduction processes may be neglected, it does appear to affect the transport properties of the other two bands through the relaxation time τ. The role of the split-off band with respect to interband scattering will be discussed in the following section.

The general form for a nonparabolic band with variable warping introduced in Sec. III contains two essential variables: The energy dependence of the warping through the parameter $b(E)$ in Eq. (5) for K^2, and the functional dependence of the energy on K^2 in Eq. (4). Thus, it is possible to obtain an exact fit to Kane's model in two directions of k space, which we choose for simplicity to be the [100] and [111] directions. For low energies this procedure reproduces the warped, parabolic bands of DKK, while for higher energies it furnishes a reasonable approximation to Kane's model in the [110] direction. The energy dependences of b and of K^2 for the light-hole band are derived from the following considerations: Since K^2 is constant over a surface of constant energy, we obtain from Eq. (4) the relations

$$k_{[100]}^2[1+b]=k_{[111]}^2[1+b(1+\tfrac{1}{3}c^2)^{1/2}]=K^2, \tag{38}$$

or, solving for b,

$$b(E)=-\frac{k_{[111]}^2-k_{[100]}^2}{(1+\tfrac{1}{3}c^2)^{1/2}k_{[111]}^2-k_{[100]}^2}. \tag{39}$$

Equations (35) and (37) are solved for $k_{[100]}^2$ and $k_{[111]}^2$ as a function of E, and the resulting expressions are substituted into Eq. (39) to obtain $b(E)$. Having obtained b as a function of E, we then substitute the appropriate relation of Eq. (38) for k^2 in terms of K^2 into either Eq. (35) or (37) to obtain $E=G(K^2)$. The resulting b versus E curve for Kane's light-hole band is shown in Fig. 7, and the G versus K^2 curve is shown in Fig. 8. The energy dependences of the quantities db/dE and $dG/d(K^2)$, which are required for the calculation of σ and $\sigma^{(H)}$ in the light-hole band, are also presented in Figs. 7 and 8, respectively.

[36] R. N. Dexter, H. J. Zeiger, and B. Lax, Phys. Rev. **104**, 637 (1956).

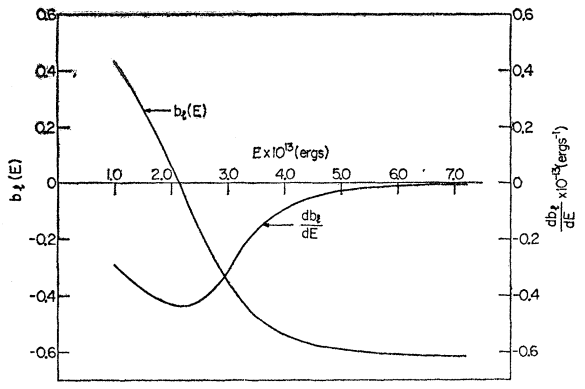

FIG. 7. Energy dependence of the warping parameter $b_l(E)$ and its derivative db_l/dE for the germanium light-hole band.

The free-hole concentrations p_h and p_l, the conductivities σ_h and σ_l, and the Hall conductivities $\sigma_h^{(H)}$ and $\sigma_l^{(H)}$ were calculated for Kane's heavy- and light-hole bands using Eqs. (14), (30), and (31). In the case of the heavy-hole band, $G(K)=AK^2$ in Eq. (4), $b=-B/A=-0.634$ in Eq. (5), $a''=1$, and $\Gamma=\gamma$. $c=C/B=1.506$ in Eq. (5) for both bands. The Hall coefficient factor r was obtained by substituting the above results into Eq. (3). Since we are interested primarily in examining the consequences of band structure with respect to the various transport properties, the relaxation times have been assumed identical for the two bands, so that they cancel in Eq. (3). Since the Hall coefficient factor is quite sensitive to the relative magnitude of the τ's, the approximate validity of this assumption can be deduced from the agreement with experiment.

The resulting theoretical prediction of r as a function of $1/Re$ is shown by the solid curve of Fig. 6. For $1/Re<5\times10^{19}$ cm^{-3}, $r>1$ and approaches the LM result for parabolic bands with constant warping. For $1/Re>5\times10^{19}$ cm^{-3}, r decreases monotonically, approaching its high-concentration value of 0.703 at $1/Re\sim3\times10^{20}$ cm^{-3}. The theoretical curve is seen to account in a quantitative way for the essential features of the experimental results.[37] Because of the experimental scatter, it is not possible to distinguish clearly any additional features which might arise from anisotropic scattering processes, the influence of the split-off band, or inequality of the two relaxation times. However, it seems clear that such effects, if they exist, must be relatively minor. The agreement between theory and experiment indicated in Fig. 6 has two significant consequences: First, it demonstrates that the Hall coefficient factor anomaly can be accounted for on the basis of appropriate band structure considerations alone. Second, it lends strong support to the validity of Kane's model for the valence band structure of germanium.

[37] After the theoretical calculations were completed, the cyclotron resonance valence band parameters quoted recently by J. J. Stickler, H. J. Zeiger, and G. S. Heller, Phys. Rev. 127, 1077 (1962), came to our attention. A calculation in the high concentration limit using their values yields $r=0.648$, which is in slightly better agreement with the experimental results.

V. DISCUSSION OF SCATTERING PROCESSES

We now turn to the question of the electronic scattering processes appropriate to degenerate p-type germanium. We have already seen that the Hall coefficient factor anomaly can be satisfactorily accounted for by proper calculation of the galvanomagnetic coefficients for the germanium valence band structure. By comparing the conductivity calculated on this basis in terms of the scattering relaxation time τ [see Eq. (30)] with the experimentally determined values presented in Fig. 2, we would expect to obtain a reliable characterization of τ as a function of energy. The resulting curves of τ versus E at $T=4.2$°K and $T=295$°K are shown in Fig. 9 for the two-band model, assuming equality of the light- and heavy-band relaxation times. For $E\lesssim0.29$ eV, τ exhibits an approximate $E^{-0.4}$ dependence at both temperatures except for a slight falloff of the 295°K curve at the lower energies. We will see that in the region of $E<0.29$ eV, τ corresponds both in energy dependence and order of magnitude to screened impurity scattering for degenerate statistics. We note that, notwithstanding the temperature dependence, the relaxation times are far too small to be accounted for on the basis of lattice scattering. For $E\gtrsim0.29$ eV, at which energy the Fermi surface first intersects the split-off band, the decrease in τ becomes much more rapid. We attribute this deterioration of the relaxation time to interband scattering involving the split-off band.

In order to obtain an estimate of the τ arising from screened impurity scattering, we consider for simplicity a spherical band of effective mass m^* in a medium of dielectric constant ϵ. The total electronic scattering cross section for momentum transfer due to a screened impurity potential of the form $V(r)=-(e^2/\epsilon r)e^{-r/\lambda}$ is,

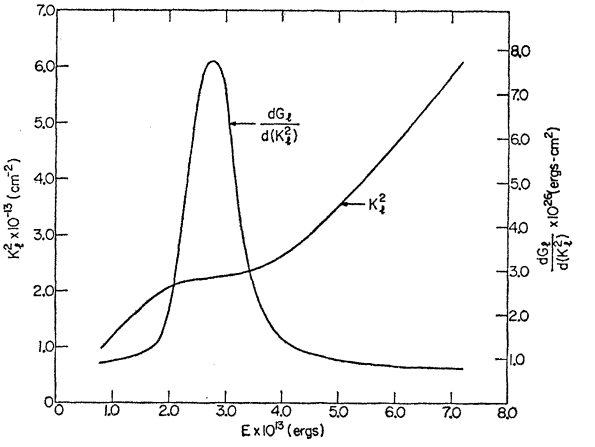

FIG. 8. Energy dependence of the quantities K^2_l and $dG_l/d(K^2_l)$, showing the nonparabolicity of the germanium light-hole band.

in the Born approximation,[38]

$$\bar{\sigma}(E)=\frac{2\pi e^4 m^{*2}}{\epsilon^2\hbar^4 k^4}\left[\ln(1+4\lambda^2k^2)-\frac{4\lambda^2k^2}{1+4\lambda^2k^2}\right], \quad (40)$$

where λ is the electronic screening radius. This is precisely the Brooks-Herring result.[39] Hence, the relaxation time due to a concentration N of impurity ions is

$$\tau(E)=\frac{m^*}{\hbar k N\bar{\sigma}}=\frac{\epsilon^2\hbar^3k^3}{2\pi e^4 m^* N}\times\left[\ln(1+4\lambda^2k^2)-\frac{4\lambda^2k^2}{1+4\lambda^2k^2}\right]^{-1}. \quad (41)$$

The quantity λ^2 is determined by the ratio of the diffusion constant D to the mobility μ according to

$$\lambda^2=(\epsilon/4\pi eN)(D/\mu). \quad (42)$$

The mobility-diffusion ratio is, in turn, determined by the Einstein relation[40]

$$\mu/eD=(1/N)(dN/dE_F), \quad (43)$$

where here E_F is the Fermi level referred to an arbitrary fixed zero of energy. By properly taking into account the energy displacement of both the Fermi level and the band edge as the semiconductor is doped to degeneracy,[41] it can be shown that[42]

$$\lambda^2=\epsilon E/10\pi e^2N, \quad (44)$$

where E is the Fermi energy referred to the band edge.

The relaxation time was calculated for the heavy-hole band from Eqs. (41) and (44), using the density-of-states effective mass $m^*=3.11\times10^{-28}$ g obtained from Eq. (14) for the heavy-hole concentration. The magnitude of the resulting τ was found to be too large by a factor ~3. Although the criterion of validity for the Born approximation is not well satisfied over the range of impurity concentrations studied, since $k\lambda$ never becomes $\gg1$, the discrepancy between the observed and predicted magnitude of τ seems too large to be adequately accounted for on this basis. We suggest, rather, that there must exist additional, related scattering processes which we have not considered. One such process may arise from the interaction between the conducting electrons and the localized electrons which screen the impurity potentials. A second process may involve, in the case of multiband degenerate semiconductors, interband impurity scattering. This latter possibility has previously been suggested by Pankove and Aigrain[9] in connection with their optical studies on degenerate material and also by Morgan.[43]

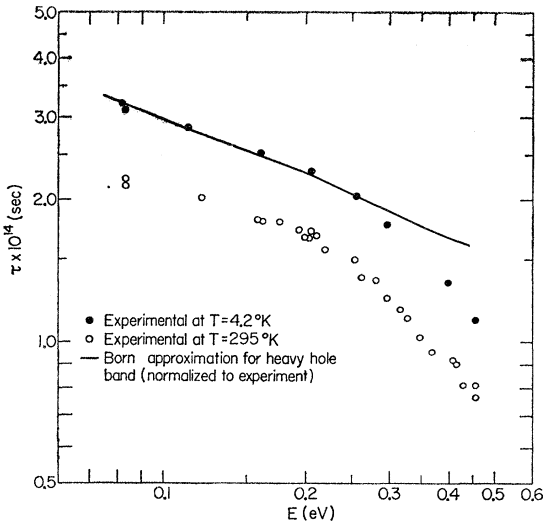

FIG. 9. Energy dependence of the average scattering relaxation time τ for the light- and heavy-hole bands at $T=4.2$°K and $T=295$°K. The marked departure from the theoretical energy dependence for $E>0.29$ eV is attributed to interband scattering involving the split-off band.

The solid curve in Fig. 9 shows the theoretical prediction of τ versus E normalized to the experimental results at $T=4.2$°K to permit a comparison with the observed energy dependence. For $E\lesssim0.29$ eV the agreement is found to be surprisingly good. However, for $E\gtrsim0.29$eV the experimental points are seen to fall off far more rapidly than the predicted curve. The fact that the Fermi surface intersects the split-off band for $E>0.29$ eV suggests that the marked depression of τ in the range of high impurity concentrations arises from the contribution of the split-off band to the scattering processes in the light- and heavy-hole bands. This conclusion is further supported by the apparent insensitivity of the Hall coefficient factor, Fig. 6, to the presence of the split-off band, in spite of its extremely low effective mass. In Appendix B we consider some general consequences of interband scattering from the point of view of the Boltzmann equation and detailed balance. It is shown that the effect of interband scattering on the relaxation of carriers in a low-mass band is considerably more pronounced than that in a high-mass band. Since, according to the analysis of Fig. 9, the interband scattering between the split-off band and the two principal bands can be quite appreciable, we would expect τ in the split-off band to be considerably smaller than that in the other two bands. This conclusion is supported by a detailed examination of Eqs. (B14) and (B15) in conjunction with results shown in Fig. 9.

[38] L. I. Schiff, *Quantum Mechanics* (McGraw-Hill Book Company, Inc., 1949), p. 168–169.
[39] H. Brooks, Phys. Rev. **83**, 879 (1951).
[40] R. Kubo, J. Phys. Soc. Japan **12**, 570 (1957).
[41] W. Bernard, H. Roth, A. P. Schmid, and P. Zeldes, Bull. Am. Phys. Soc. **7**, 232 (1962); also Phys. Rev. **131**, 627 (1963).
[42] The expression for λ^2 given by Eq. (44) can be shown to be valid for a system of parabolic bands having a common zero of energy. Furthermore, we note that for the conventional calculation of λ^2, in which the motion of the band edges is ignored, the factor $\frac{1}{10}$ is replaced by $\frac{1}{6}$.
[43] T. N. Morgan, Bull. Am. Phys. Soc. **8**, 224 (1963).

The temperature dependence of the resistivity shown in Fig. 3, and the corresponding temperature dependence of the scattering relaxation time indicated in Fig. 9, also raise fundamental questions with respect to the electronic screening of impurity ions in a degenerate semiconductor. In the range of degenerate statistics it seems reasonable to attribute the temperature dependence of the relaxation time to that of the screening radius λ [see Eq. (41)]. We have observed a similar temperature dependence of the screening radius in connection with our junction potential studies in germanium tunnel diodes.[41] The junction capacitance built-in voltage, which contains a negative term $\propto\lambda^2$, exhibits, as in the case of τ, a saturation with temperature for $T<80°$K and a monotonic decrease with increasing temperature for $T>80°$K. Furthermore, the relative magnitude of the observed changes with temperature of the capacitance built-in voltage of the diodes and the relaxation time in the bulk material appears to be consistent with the assumption of a common temperature-dependent λ. However, the proposed temperature dependence of the electronic screening radius cannot be readily accounted for. Although, as the temperature is increased, one would indeed expect the screening to become less effective due to enhanced thermal motion of the free carriers, no appreciable increase in λ should occur so long as kT remains small compared to the Fermi energy.

In addition, the origin of the interband scattering by screened impurity potentials is not apparent on the basis of conventional scattering theory. The role of phonons with respect to momentum conservation in interband scattering has been extensively studied by Herring[1] and others and is well understood. However, the mechanism by which crystal momentum can be conserved in interband scattering by screened impurity ions is by no means clear. This, as well as the question of the temperature dependence of the electronic screening radius, remains an interesting problem for future investigation.

ACKNOWLEDGMENTS

We would like to acknowledge the interest of R. Tramposch and Dr. J. Patel, whose questions concerning the Hall coefficient factor in degenerate semiconductors originally prompted the present work. We thank them also for providing the great wealth of carefully grown crystals used in these investigations. Particular thanks are due to M. Lichtensteiger, who adapted the EDTA complexometric titration method to the gallium-germanium system. Finally, we are indebted to Miss M. Harrison, Mrs. B. Mikulec, and Miss W. Doherty for performing the detailed calculations.

APPENDIX A

In this Appendix we derive the expression, Eq. (18), for the term in the integrand of Eq. (12) involving s econd derivatives of E with respect to k.

Differentiation of Eq. (15) for $\partial E/\partial k_x$ with respect to k_x yields

$$\frac{\partial^2 E}{\partial k_x^2}=\frac{d^2G}{d(K^2)^2}\left[\frac{D(K^2)}{Dk_x}+\frac{db}{dE}\frac{\partial E}{\partial k_x}\Lambda^2\right]^2+\frac{dG}{d(K^2)}\left[\frac{D^2(K^2)}{Dk_x^2}+2\frac{db}{dE}\frac{\partial E}{\partial k_x}\frac{k_xM_x^2}{\Lambda^2}+\frac{d^2b}{dE^2}\left(\frac{\partial E}{\partial k_x}\right)^2\Lambda^2+\frac{db}{dE}\frac{\partial^2 E}{\partial k_x^2}\Lambda^2\right], \tag{A1}$$

where

$$M_x^2=2k^2+c^2(k_y^2+k_z^2). \tag{A2}$$

Similarly, differentiation of Eq. (15) with respect to k_y yields

$$\frac{\partial^2 E}{\partial k_x\partial k_y}=\frac{d^2G}{d(K^2)^2}\left[\frac{D(K^2)}{Dk_x}+\frac{db}{dE}\frac{\partial E}{\partial k_x}\Lambda^2\right]\left[\frac{D(K^2)}{Dk_y}+\frac{db}{dE}\frac{\partial E}{\partial k_y}\Lambda^2\right]$$
$$+\frac{dG}{d(K^2)}\left[\frac{D^2(K^2)}{Dk_xDk_y}+\frac{1}{\Lambda^2}\frac{db}{dE}\left(k_xM_x^2\frac{\partial E}{\partial k_y}+k_yM_y^2\frac{\partial E}{\partial k_x}\right)+\frac{d^2b}{dE^2}\frac{\partial E}{\partial k_x}\frac{\partial E}{\partial k_y}\Lambda^2+\frac{db}{dE}\frac{\partial^2 E}{\partial k_x\partial k_y}\Lambda^2\right], \tag{A3}$$

where

$$M_y^2=2k^2+c^2(k_z^2+k_x^2). \tag{A4}$$

Substituting for $\partial E/\partial k_x$ and $\partial E/\partial k_y$ from Eq. (17) and solving Eqs. (A1) and (A3) for $\partial^2 E/\partial k_x^2$ and $\partial^2 E/\partial k_x\partial k_y$,

respectively, we obtain

$$\frac{\partial^2 E}{\partial k_x^2}=\left\{\frac{1}{1-(db/dE)[dG/d(K^2)]\Lambda^2}\right\}\left\{\frac{d^2G}{d(K^2)^2}\left[\frac{D(K^2)/Dk_x}{1-(db/dE)[dG/d(K^2)]\Lambda^2}\right]^2\right.$$
$$+\frac{dG}{d(K^2)}\left[\frac{D^2(K^2)}{Dk_x^2}+2\frac{k_xM_x^2}{\Lambda^2}\frac{db}{dE}\frac{dG}{d(K^2)}\frac{D(K^2)}{Dk_x}\Big/\left(1-\frac{db}{dE}\frac{dG}{d(K^2)}\Lambda^2\right)\right.$$
$$\left.\left.+\Lambda^2\frac{d^2b}{dE^2}\left(\frac{dG}{d(K^2)}\frac{D(K^2)}{Dk_x}\Big/\left(1-\frac{db}{dE}\frac{dG}{d(K^2)}\Lambda^2\right)\right)^2\right]\right\} \quad \text{(A5)}$$

and

$$\frac{\partial^2 E}{\partial k_x\partial k_y}=\left\{1\Big/\left[1-\frac{db}{dE}\frac{dG}{d(K^2)}\Lambda^2\right]\right\}\left\{\frac{d^2G}{d(K^2)^2}\frac{D(K^2)}{Dk_x}\frac{D(K^2)}{Dk_y}\Big/\left(1-\frac{db}{dE}\frac{dG}{d(K^2)}\Lambda^2\right)^2\right.$$
$$+\frac{dG}{d(K^2)}\left[\frac{D^2(K^2)}{Dk_xDk_y}+\frac{db}{dE}\frac{dG}{d(K^2)}\left(k_xM_x^2\frac{D(K^2)}{Dk_y}+k_yM_y^2\frac{D(K^2)}{Dk_x}\right)\Big/\Lambda^2\left(1-\frac{db}{dE}\frac{dG}{d(K^2)}\Lambda^2\right)\right.$$
$$\left.\left.+\Lambda^2\frac{d^2b}{dE^2}\left(\frac{dG}{d(K^2)}\right)^2\frac{D(K^2)}{Dk_x}\frac{D(K^2)}{Dk_y}\Big/\left(1-\frac{db}{dE}\frac{dG}{d(K^2)}\Lambda^2\right)^2\right]\right\}. \quad \text{(A6)}$$

We now substitute Eqs. (A5) and (A6), together with Eq. (17) for $\partial E/\partial k_x$ and $\partial E/\partial k_y$, into the quantity

$$\left[\left(\frac{\partial E}{\partial k_y}\right)^2\frac{\partial^2 E}{\partial k_x^2}-\frac{\partial E}{\partial k_x}\frac{\partial E}{\partial k_y}\frac{\partial^2 E}{\partial k_x\partial k_y}\right].$$

This procedure yields

$$\left(\frac{\partial E}{\partial k_y}\right)^2\frac{\partial^2 E}{\partial k_x^2}-\frac{\partial E}{\partial k_x}\frac{\partial E}{\partial k_y}\frac{\partial^2 E}{\partial k_x\partial k_y}=\left\{\frac{dG/d(K^2)}{1-(db/dE)[dG/d(K^2)]\Lambda^2}\right\}^3\left\{\left[\left(\frac{D(K^2)}{Dk_y}\right)^2\frac{D^2(K^2)}{Dk_x^2}-\frac{D(K^2)}{Dk_x}\frac{D(K^2)}{Dk_y}\frac{D^2(K^2)}{Dk_xDk_y}\right]\right.$$
$$\left.+\frac{(db/dE)[dG/d(K^2)]}{\Lambda^2(1-(db/dE)[dG/d(K^2)]\Lambda^2)}\left[k_xM_x^2\left(\frac{D(K^2)}{Dk_y}\right)^2\frac{D(K^2)}{Dk_x}-k_yM_y^2\left(\frac{D(K^2)}{Dk_x}\right)^2\frac{D(K^2)}{Dk_y}\right]\right\}, \quad \text{(A7)}$$

all other terms canceling identically. However, since all other factors appearing in the integrand of Eq. (12) possess cubic symmetry, we are free to interchange x and y in any term in Eq. (A7). Therefore, the terms involving $k_xM_x^2$ and $k_yM_y^2$ cancel, and Eq. (A7) reduces to Eq. (18).

APPENDIX B

We consider here certain general features of interband scattering from the point of view of the Boltzmann equation and detailed balancing. In particular, we shall derive expressions for the scattering relaxation times τ_1 and τ_2 appropriate to a system of two spherically symmetric bands in terms of the interband scattering cross sections.

To first order in the electric field $\mathcal{E}$, and zero order in the magnetic field, the Boltzmann equation for band 1 can be written in the form

$$e(\partial f_0/\partial E)\mathcal{E}\cdot\mathbf{v}_1$$
$$=-\Delta f(\mathbf{k}_1)\int d\mathbf{k}_1'\,P(\mathbf{k}_1,\mathbf{k}_1')+\int d\mathbf{k}_1'\,\Delta f(\mathbf{k}_1')P(\mathbf{k}_1',\mathbf{k}_1)$$
$$-\Delta f(\mathbf{k}_1)\int d\mathbf{k}_2'\,P(\mathbf{k}_1,\mathbf{k}_2')$$
$$+\int d\mathbf{k}_2'\,\Delta f(\mathbf{k}_2')P(\mathbf{k}_2',\mathbf{k}_1), \quad \text{(B1)}$$

where $\Delta f(k_i)$ is the displacement of the distribution function in the ith band from its equilibrium value f_0, $P(\mathbf{k}_i,\mathbf{k}_j)$ is the transition rate from $\mathbf{k}_i$ to $\mathbf{k}_j$, and $\mathbf{v}_i=(1/\hbar)\nabla_{k_i}E$ is the electron velocity in the state $\mathbf{k}_i$. Similarly, the Boltzmann equation for band 2 is

$$e(\partial f_0/\partial E)\mathcal{E}\cdot\mathbf{v}_2$$
$$=-\Delta f(\mathbf{k}_2)\int d\mathbf{k}_2'\,P(\mathbf{k}_2,\mathbf{k}_2')+\int d\mathbf{k}_2'\,\Delta f(\mathbf{k}_2')P(\mathbf{k}_2',\mathbf{k}_2)$$
$$-\Delta f(\mathbf{k}_2)\int d\mathbf{k}_1'\,P(\mathbf{k}_2,\mathbf{k}_1')$$
$$+\int d\mathbf{k}_1'\,\Delta f(\mathbf{k}_1')P(\mathbf{k}_1',\mathbf{k}_2). \quad \text{(B2)}$$

We assume that the scattering centers are spherically symmetric and that the electronic energy is conserved in the scattering process. Then the transition rate $P(\mathbf{k}_i,\mathbf{k}_j')$ can be written in terms of the corresponding

differential cross section $\sigma_{ij}(\theta_{ij'})$ according to

$$P(\mathbf{k}_i,\mathbf{k}_j')=(N\hbar v_i v_j/k_j^2)\sigma_{ij}(\theta_{ij'})\delta(E_i-E_j'), \quad \text{(B3)}$$

where $\theta_{ij'}$ denotes the angle between $\mathbf{k}_i$ and $\mathbf{k}_j'$, and N is the concentration of scattering centers. If, in addition, we make the physically reasonable assumption that the interband and intraband scattering transition rates separately obey the detailed balance condition

$$P(\mathbf{k}_i,\mathbf{k}_j')=P(\mathbf{k}_j',\mathbf{k}_i), \quad \text{(B4)}$$

then it follows from Eq. (B3) that

$$\sigma_{ij}(\theta)=(k_j^2/k_i^2)\sigma_{ji}(\theta). \quad \text{(B5)}$$

Substituting for P in terms of σ_{ij} from Eq. (B3), the Boltzmann Eqs. (B1) and (B2) become

$$\begin{aligned}e\frac{\partial f_0}{\partial E}\mathcal{E}\cdot\mathbf{v}_1=&-Nv_1\Delta f(\mathbf{k}_1)\int d\Omega_1'\,\sigma_{11}(\theta_{11'})\\&+Nv_1\int d\Omega_1'\,\Delta f(\mathbf{k}_1')\sigma_{11}(\theta_{11'})\\&-Nv_1\Delta f(\mathbf{k}_1)\int d\Omega_2'\,\sigma_{12}(\theta_{12'})\\&+Nv_1\frac{k_2^2}{k_1^2}\int d\Omega_2'\,\Delta f(\mathbf{k}_2')\sigma_{21}(\theta_{12'}) \quad \text{(B6)}\end{aligned}$$

and

$$\begin{aligned}e\frac{\partial f_0}{\partial E}\mathcal{E}\cdot\mathbf{v}_2=&-Nv_2\Delta f(\mathbf{k}_2)\int d\Omega_2'\,\sigma_{22}(\theta_{22'})\\&+Nv_2\int d\Omega_2'\,\Delta f(\mathbf{k}_2')\sigma_{22}(\theta_{22'})\\&-Nv_2\Delta f(\mathbf{k}_2)\int d\Omega_1'\,\sigma_{21}(\theta_{21'})\\&+Nv_2\frac{k_1^2}{k_2^2}\int d\Omega_1'\,\Delta f(\mathbf{k}_1')\sigma_{12}(\theta_{21'}), \quad \text{(B7)}\end{aligned}$$

where $d\Omega$ denotes an elementary solid angle. By expanding σ_{ij} in Legendre polynomials and invoking the addition law for spherical harmonics, it is readily verified that Eqs. (B6) and (B7) are satisfied by solutions of the form

$$\Delta f(\mathbf{k}_i)=\chi_i(E)\cos\theta_i, \quad \text{(B8)}$$

where θ_i is the angle between $\mathcal{E}$ and $\mathbf{k}_i$. In fact, substitution of Eq. (B8) into Eqs. (B6) and (B7) yields

$$e\frac{\partial f_0}{\partial E}\mathcal{E}v_1=-\chi_1(E)\left(\frac{1}{\tau_{11}}+\frac{1}{{}_1\tau_{12}}\right)-\chi_2(E)\frac{1}{{}_2\tau_{12}} \quad \text{(B9)}$$

and

$$e\frac{\partial f_0}{\partial E}\mathcal{E}v_2=-\chi_2(E)\left(\frac{1}{\tau_{22}}+\frac{1}{{}_1\tau_{21}}\right)-\chi_1(E)\frac{1}{{}_2\tau_{21}}, \quad \text{(10)}$$

where

$$\frac{1}{\tau_{ii}}=Nv_i\int d\Omega\,(1-\cos\theta)\sigma_{ii}(\theta) \quad \text{(B11)}$$

and

$$\frac{1}{{}_1\tau_{ij}}=Nv_i\int d\Omega\,\sigma_{ij}(\theta), \quad \frac{1}{{}_2\tau_{ij}}=-Nv_i\int d\Omega\,\cos\theta\sigma_{ij}(\theta)$$

$$\text{for } i\neq j. \quad \text{(B12)}$$

We note that $|1/{}_2\tau_{ij}|<|1/{}_1\tau_{ij}|$, and that for s-wave scattering $1/{}_2\tau_{ij}=0$.

Solving Eqs. (B9) and (B10) for $\Delta f(\mathbf{k}_i)=\chi_i(E)\cos\theta_i$, we obtain

$$\Delta f(\mathbf{k}_i)=-e(\partial f_0/\partial E)\mathbf{v}_i\cdot\mathcal{E}\tau_i, \quad \text{(B13)}$$

where

$$\tau_i=\frac{\dfrac{1}{\tau_{jj}}+\dfrac{1}{{}_1\tau_{ji}}\dfrac{v_j}{v_i}\dfrac{1}{{}_2\tau_{ij}}}{\left[\left(\dfrac{1}{\tau_{ii}}+\dfrac{1}{{}_1\tau_{ij}}\right)\left(\dfrac{1}{\tau_{jj}}+\dfrac{1}{{}_1\tau_{ji}}\right)-\dfrac{1}{{}_2\tau_{ij}}\dfrac{1}{{}_2\tau_{ji}}\right]}. \quad \text{(B14)}$$

By invoking the detailed balance condition of Eq. (B5), together with the definitions of Eq. (B12), we find

$$\frac{1}{{}_m\tau_{ij}}=\frac{v_i}{v_j}\frac{k_j^2}{k_i^2}\frac{1}{{}_m\tau_{ji}} \quad \text{for } m=1,2, \quad \text{(B15)}$$

which implies that the effect of interband scattering on the lifetime in a light hole band will be more pronounced than that on the lifetime in a heavy-hole band. A quantitative estimate of the effect of interband scattering for any specific model can be obtained in principle using Eqs. (B14) and (B15).